TECHNICAL TRANSACTIONS | **CZASOPISMO TECHNICZNE**
CHEMISTRY | CHEMIA
2-Ch/2014

ŁUKASZ KACPERSKI*, JOANNA KARCZ*

CFD METHOD FOR EVALUATION OF CRITICAL IMPELLER SPEED REQUIRED FOR FLOATING PARTICLES SUSPENSION

ZASTOSOWANIE METODY CFD DO OCENY KRYTYCZNYCH CZĘSTOŚCI OBROTÓW MIESZADŁA PODCZAS WYTWARZANIA ZAWIESINY LEKKIEJ

Abstract

In the paper, critical impeller speeds were analyzed on the basis of the performed simulations of the concentration distribution of the floating particles suspension in an agitated vessel, equipped with pitched blade turbine. The required range of the standard deviation of the local particles concentration in a suspension was assumed as comparative criterion. The results obtained from numerical computations were compared with the values of the critical impeller speeds determined experimentally.

Keywords: *CFD method*, *suspension of floating particles*, *critical impeller speed*

Streszczenie

W artykule analizowano krytyczne częstości obrotów mieszadła na podstawie wykonanych symulacji rozkładu stężeń zawiesiny cząstek lekkich w zbiorniku z mieszadłem turbinowym o łopatkach pochylonych. Jako kryterium porównawcze przyjęto wymagany zakres wartości odchylenia standardowego stężeń lokalnych cząstek w zawiesinie. Wyniki uzyskane z obliczeń numerycznych porównano z wartościami krytycznych częstości obrotów mieszadła określonymi doświadczalnie.

Słowa kluczowe: *metoda CFD*, *zawiesina cząstek lekkich*, *krytyczna częstość obrotów*

* M.Sc. Eng. Łukasz Kacperski, Prof. Joanna Karcz, Department of Chemical Engineering, Faculty of Chemical Engineering, West Pomeranian University of Technology, Szczecin.

1. Introduction

Operation of the drawdown of floating particles in an agitated liquid is often used, for example, in food processing fermentation or wastewater treatment. Solid particles less dense than the liquid will float onto the liquid surface when such solid–liquid system will not sufficiently mechanically agitated [1–2]. Experimental results concerning dispersion of floating particles in an agitated vessel are presented in few papers [3–8]. Recently, CFD methods are also used to analyze fluid flow and concentration fields for mechanically agitated suspensions of the floating particles [9–16]. Numerical simulations of the distribution of the particles concentration for solid–liquid system with floating particles were carried out by Murthy et al. [10], Cekinski et al. [11] and Tamburini et al. [13]

The aim of the study presented in this paper was to evaluate critical impeller speed on the basis of the performed simulations of the concentration distributions of the floating particles suspension in an agitated vessel. Assuming required level of the standard deviation σ of the particle concentration as comparative criterion, values of the impeller speeds were analyzed.

2. Range of numerical simulations

Numerical simulations were carried out for a solid – liquid system agitated in a flat--bottomed baffled vessel with inner diameter $D = 0.295$ m. The vessel was filled with a fluid to height $H = D$. Up-pumping pitched blade turbine with six blades ($\alpha = 45°$) with impeller diameter $d = 0.33D$ was located at height $h = 0.67H$ from the vessel bottom. The agitated vessel was equipped with four standard planar baffles.

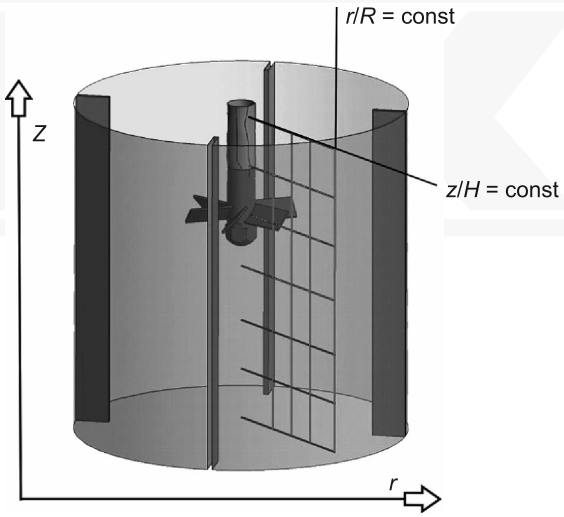

Fig. 1. Scheme of the agitated vessel used in the study and sampling coordinate of local values of the particles concentration x at axial and radial planes (coordinates z/H and r/R)

Distilled water was used as liquid phase. Particles of polyethylene with density ρ_p = 952 kg/m^3 and average diameter d_p = 0.0038 m were applied as solid phase. Three different mean concentrations x_m of the particles in a suspension, equal to 1.042×10^{-2}; 5.224×10^{-2}; or 10.423×10^{-2} vol. fraction (corresponding to the mass. concentration X_m equal to 1%, 5% or 10%, respectively) were tested. For each concentration value, numerical computations were carried out within the range of the impeller speeds $n \in \langle 0.99; 6.42 \rangle$ 1/s.

Numerical simulations were carried out using ANSYS CFX 13.0 [17] and unstructural grid with ca. 121 000 nodes (ca. 659 000 of tetrahedral elements). Quality of numerical grid was checked out in previous studies [15]. *Shear Stress Transport* turbulence model with automatic wall function was used. This turbulence model contains blending functions for $k - \varepsilon$ and $k - \omega$ turbulence models. For simulations refer to 1% particles concentration, *Particle* model with drag force equation proposed by Wen and Yu [17] was taken into account, whereas Gidaspow drag force model [17] was used in case of simulations concerning 5% and 10% particles concentration. *Multiple Reference Frame* model was implemented to simulate a rotational movement of impeller for quasi-steady process.

3. Results

Based on the numerical data of the concentration field, local values of the polyethylene particles concentration x as a function of the dimensionless axial z/H and radial r/R (where $R = D/2$) coordinates were determined for different values of the impeller speed n and mean mass concentration X_m. An example of the axial normalized distributions of the particles concentration in the form of the graph $x/x_m = f(z/H)$ is presented in Fig. 2 for mean concentration of the particles equal to 5% mass. These profiles describe three levels of the normalized radial coordinate r/R equal to: 0.34 (region located the nearest blades of the impeller, Fig. 2a), 0.5 (region located in the middle between impeller blades and vessel wall, Fig. 2b) and 0.73 (Fig. 2c), respectively. Empty circles in Figs. 2a, 2b and 2c correspond to the value of the just drawdown speed n_{JD} determined experimentally by Karcz and Mackiewicz [5–8]. The value x/x_m equal to one is characteristic for such state of the suspension in the volume of the vessel where local particles concentration x corresponds to mean value of the particles concentration x_m in the agitated vessel. As it is shown in Fig. 2a, normalized local values of the concentration x/x_m are lower than one for each of the n value and range of the axial coordinate $z/H < 0.95$. The x/x_m values reach unit within the range $z/H \in (0.5; 0.95)$ for the dimensionless radial coordinate $r/R = 0.51$ (Fig. 2b), as well as within the range $z/H \in (0.35; 0.95)$ for the $r/R = 0.73$ (Fig. 2c). Axial extension of the zones with the values x/x_m higher than one for the concentrations profiles shown in Figs. 2a, 2b and 2c is caused by fluid circulation imposed by up-pumping pitched blade turbine. In this case, fluid stream more intensively surrounds vessel wall than impeller shaft.

Radial distributions of the dimensionless particles concentration x/x_m for a given level of the dimensionless axial coordinate z/H = const and mean particles concentration X_m = 5% mass. are shown in Fig. 3. Level of the $z/H = 0.33$ corresponds to the zone below the impeller and it is located relatively close to the vessel bottom (Fig. 3a), level of the $z/H = 0.5$ is ascribed to the middle of the liquid height in the vessel (Fig. 3b) and $z/H = 0.67$

corresponds to the off-bottom clearance of the impeller (Fig. 3c). For the z/H = 0.33, local homogeneity of the suspension equal to mean concentration of the particles in the vessel is reached for the radial coordinate r/R somewhat higher than 0.75 (Fig. 3a). The x/x_m values rapidly increase up to $x/x_m \approx 2$ within the range of $r/R \in (0.75; 1)$ and they softly change from one to zero within the range of $r/R \in (0.75; 0)$. For the axial coordinate z/H = 0.5, the point for which $x/x_m = 1$ is described by radial coordinate r/R equal about of 0.65 (Fig. 3b). Therefore, relocation of the point $x/x_m = 1$ is observed at the direction of the smaller values of the r/R coordinate with the increase of the z/H coordinate. For the z/H = 0.5, lower differences between the highest values x/x_m in both zones described by means of the r/R intervals, i.e. $r/R \in (0; 0.65)$ and $r/R \in (0.65; 1)$ are observed (Fig. 3b). As Fig. 3c shows, profiles of $x/x_m = f(r/R)$ for the level of the impeller location (z/H = 0.67) are the asymmetric curves with the maximum ascribed to the radial coordinate r/R equal about of 0.8. In this case, the value of $x/x_m = 1$ is reached for the coordinate r/R equal about of 0.5.

Standard deviation σ of the particles concentration along axial coordinate z/H was calculated for a given value of the radial coordinate r/R. Four different values of the radial coordinate r/R equal to 0.34; 0.52; 0.73 and 0.99, respectively, were taken into account in the computations. More over, analogous calculations of the standard deviation were carried out along radial coordinate r/R for a given value of the axial coordinate. Seven different values of the axial coordinate z/H are considered within the range $z/H \in \langle 3.39 \times 10^{-2}; 0.97\rangle$.

Computations of the standard deviation σ were performed according to the following definition

$$\sigma = \sqrt{\frac{1}{N}\sum_{N=1}^{i}\left(\frac{x_i - x_m}{x_m}\right)^2} \tag{1}$$

where:

x_i – i-th value of the particle concentration (vol. fraction),
x_m – mean value of the particles concentration (vol. fraction),
N – number of sampling points.

Values of the standard deviation σ were computed for the mean particles concentration X_m equal to 1%, 5% and 10% mass. For a given X_m value, σ values were calculated for the experimentally determined [5–7], critical impeller speed n_{JD}, as well as for the other impeller speeds n. Standard deviation σ estimated along the axial coordinate z/H for assumed r/R = const (vertical line, Fig. 1) was calculated on the basis of the N = 60 numerical data of the x values, whereas analogous computations performed along the radial coordinate r/R for assumed z/H = const (horizontal line, Fig. 1) were conducted on the basis of the N = 30 points. The obtained results of the σ values for the mean concentration of the particles equal to 5% are collected in Tables 1 and 2. The data in Table 1 show that, for the r/R = const, standard deviation σ decreases with the increase of the impeller speed n. The σ values behave analogously for the z/H = const (Table 2). For the just drawdown impeller speed n_{JD} (bolded values in Tables 1 and 2), mean value of the σ is equal to 0.61 within the range of the $r/R \in \langle 0.34; 0.99\rangle$ (Table 1) and σ = 0.66 within the range z/H <0.18; 0.82> (Table 2).

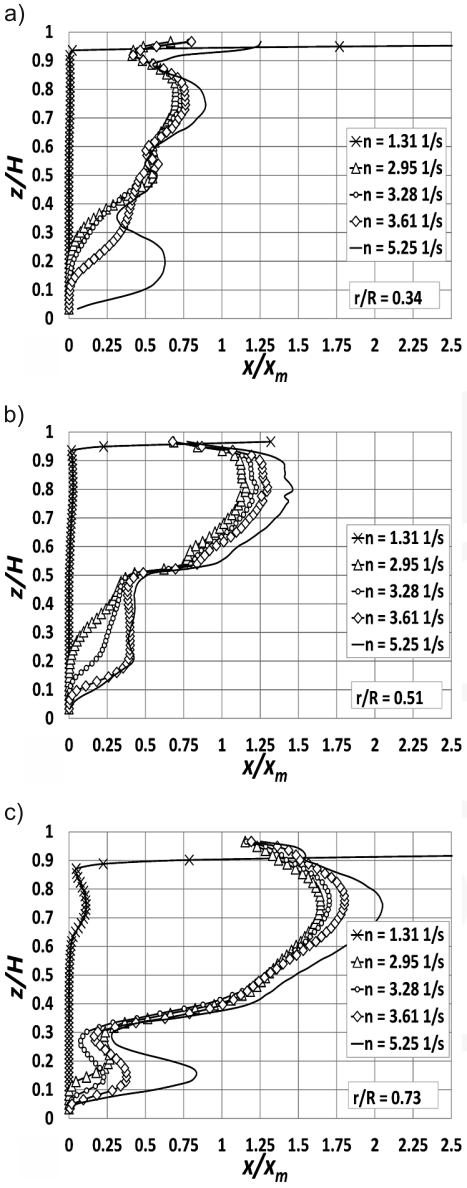

Fig. 2. Axial profiles $x/x_m = f(z/H)$ for different impeller speeds n and mean concentration of the particles X_m = 5% mass.; (where x, x_m – particles concentration in vol. fraction); a) r/R = 0.34; b) r/R = 0.51; c) r/R = 0.73

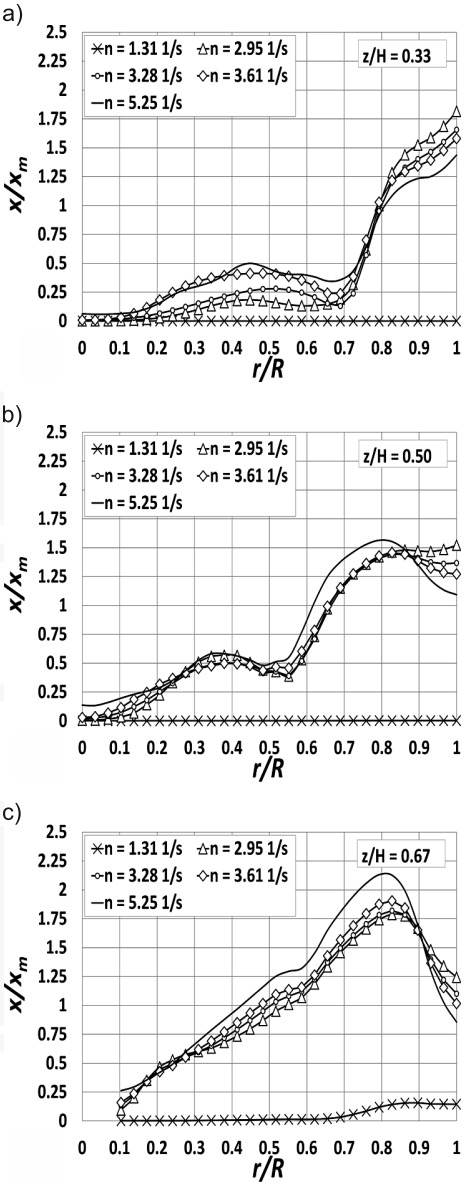

Fig. 3. Radial profiles $x/x_m = f(r/R)$ for different impeller speeds n and mean concentration of the particles X_m = 5% mass.; (where x, x_m – particles concentration in vol. fraction); z/H = 0.34; b) z/H = 0.50; c) z/H = 0.67

In case of the data in Table 2, extreme values of the σ were not taken into account for the calculation of the averaged value. Both σ values correspond to the range $0.2 < \sigma < 0.8$ which is proposed by Cekinski et al. [12] as a criterion of the enough particles dispersion in the suspension.

Dependences of the standard deviation σ on the impeller speed n are compared in Figs. 4 and 5 for three values of the mass. concentration X_m of the particles, equal to 1%, 5% and 10%, respectively. In Figs. 4 and 5, the region corresponding to the criterion $0.2 < \sigma < 0.8$ is distinguished by grey colour. Experimentally determined values of the just drawdown impeller speeds are equal to $n_{JD} = 2.47$ 1/s, $n_{JD} = 3.28$ 1/s and $n_{JD} = 4.01$ 1/s [5–8], respectively, for the particles concentration 1%, 5% and 10% mass. As Figs. 4 and 5 show, all these n_{JD} values are located within the range of the $0.2 < \sigma < 0.8$.

Fig. 4 presents the dependence of the standard deviation σ on the impeller speed n for the data from Table 1 calculated for the given dimensionless radial coordinate r/R equal to 0.51 (Fig. 4a) or 0.73 (Fig. 4b). In the zones, where impeller speeds are lower than n_{JD}, the σ values increase with the increase of the particles concentration X_m (% mass.). In Fig. 5, the dependence $\sigma = f(n)$ is shown for the data from Table 2 calculated for the given dimensionless coordinate z/H equal to 0.33 (Fig. 5a) or 0.67 (Fig. 5b). The zone corresponding to the level $z/H = 0.33$ is located at near distance from the vessel bottom and far from the impeller, therefore, agitation in this region is less intensive and particles are weakly dispersed in the liquid compared to the impeller zone ($z/H = 0.67$). Values of the standard deviation σ for the impeller zone (Fig. 5b) are smaller than those for the level $z/H = 0.33$ (Fig. 5a).

Table 1

Values of the standard deviation σ for the particles concentration along the vertical lines z/H located at the distance r/R; mean particles concentration X_m = 5% mass.; impeller speed n [1/s] ∈ <1.31; 5.25>

Vertical line z/H (N = 60 points)	r/R	n, 1/s (% relative to critical impeller speed n_{JD})										
		1.31 (–60)	2.30 (–30)	2.79 (–15)	2.95 (–10)	3.12 (–5)	**3.28** (0)	3.44 (+5)	3.61 (+10)	3.77 (+15)	4.26 (+30)	5.25 (+60)
		σ										
1	0.34	1.23	0.75	0.66	0.69	0.70	**0.67**	0.64	0.62	0.60	0.56	0.45
2	0.51	0.98	0.72	0.64	0.65	0.65	**0.60**	0.56	0.53	0.49	0.49	0.53
3	0.73	2.38	0.77	0.59	0.61	0.65	**0.65**	0.63	0.63	0.62	0.61	0.68
4	0.99	2.99	1.13	0.62	0.56	0.55	**0.52**	0.49	0.48	0.46	0.44	0.32

In Figs. 6 and 7, the dependences $\sigma = f(n)$ are compared for different values of the mean concentration X_m (% mass.) of the particles. Fig. 6 illustrates the values of the standard deviation σ obtained for a given level of the r/R coordinate, whereas σ values for a given level of the z/H coordinate are shown in Fig. 7. Fig. 6 presents the results of the numerical data for two levels of the r/R coordinate equal to 0.51 and 0.73 and for the X_m = 1% (Fig. 6a), 2% (Fig. 6b) and 10% (Fig. 6c).

Table 2

Values of the standard deviation σ for the particles concentration along the horizontal lines r/R located at the level z/H; mean particles concentration X_m = 5% mass.; impeller speed n [1/s] ∈ <1.31; 5.25>

Horizontal line r/R (N = 30 points)	z/H	n, 1/s (% relative to critical impeller speed n_{JD})										
		1.31 (–60)	2.30 (–30)	2.79 (–15)	2.95 (–10)	3.12 (–5)	**3.28** (0)	3.44 (+5)	3.61 (+10)	3.77 (+15)	4.26 (+30)	5.25 (+60)
		σ										
1	0.03	1.00	1.00	1.00	1.00	1.00	**1.00**	1.00	0.99	0.98	0.97	0.96
2	0.18	1.00	1.00	0.86	0.91	0.92	**0.89**	0.88	0.85	0.82	0.79	0.57
3	0.33	1.00	0.97	0.79	0.81	0.82	**0.77**	0.71	0.68	0.66	0.56	0.64
4	0.50	1.00	0.85	0.59	0.61	0.63	**0.59**	0.58	0.57	0.58	0.49	0.54
5	0.67	0.95	0.68	0.52	0.50	0.50	**0.50**	0.51	0.53	0.53	0.54	0.61
6	0.82	0.92	0.68	0.55	0.54	0.54	**0.55**	0.57	0.59	0.57	0.59	0.78
7	0.97	1.00	1.00	1.00	1.00	1.00	**1.00**	1.00	1.00	1.00	1.00	1.00

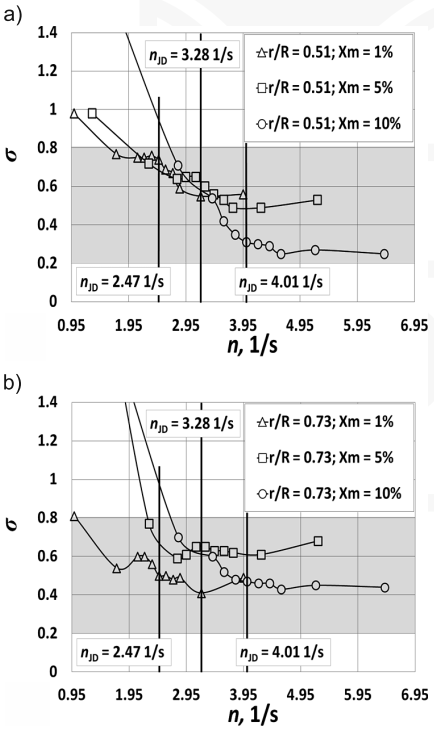

Fig. 4. The dependence $\sigma = f(n)$ for different values of the mean concentration X_m = 1; 5; 10% mass.; a) r/R = 0.51; b) r/R = 0.73

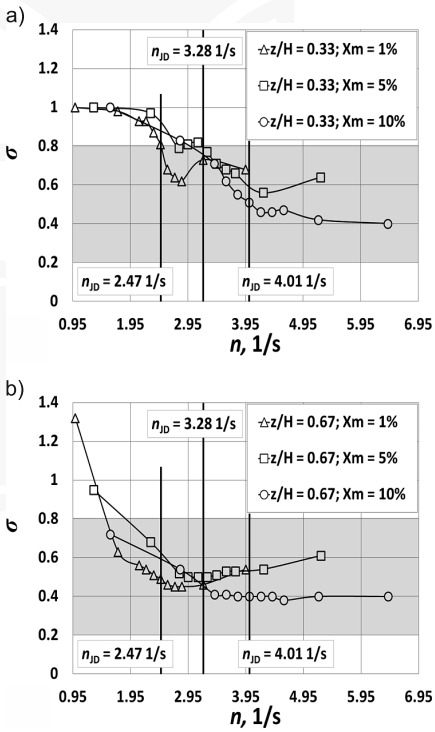

Fig. 5. The dependence $\sigma = f(n)$ for different values of the mean concentration X_m = 1; 5; 10% mass.; a) z/H = 0.33; b) z/H = 0.67

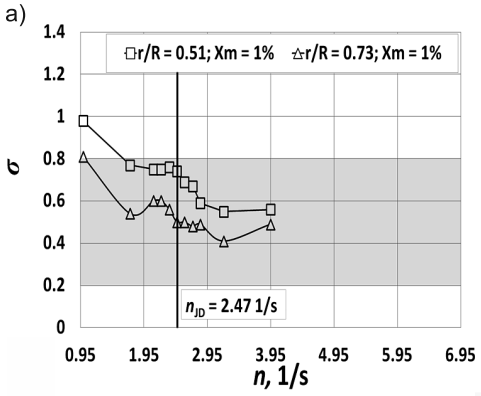

Fig. 6. The dependence $\sigma = f(n)$ for different values of the *r/R* coordinate and a given value of mean concentration X_m; a) X_m = 1% mass.; b) X_m = 5% mass.; c) X_m = 10% mass.

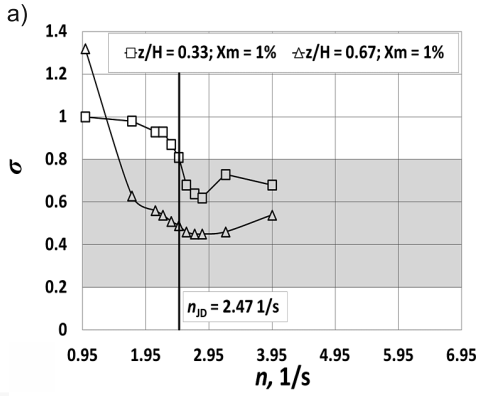

Fig. 7. The dependence $\sigma = f(n)$ for different values of the *z/H* coordinate and a given value of mean concentration X_m; a) X_m = 1% mass.; b) X_m = 5% mass.; c) X_m = 10% mass.

In case of the particles concentration equal to 1% (Fig. 6a), higher homogeneity of the suspension corresponds to the level of the radial coordinate $r/R = 0.73$ (smaller values of the σ). This tendency reverses for the higher values of the particles concentration X_m, where smaller values of the σ describe the cross-section of $r/R = 0.51$ for the values of the speeds $n \geq n_{JD}$ (Figs. 6b and 6c). The data presented in Fig. 7 show that higher homogeneity of the suspension (smaller σ values) is obtained for the impeller zone ($z/H = 0.67$) compared to that for the zone under impeller ($z/H = 0.33$) for all the values of the particles concentration X_m.

4. Conclusions

The results, obtained within the range of the performed numerical computations, show that:

1. Consistence of the experimental and numerical results demonstrates that CFD method can be successfully applied to analyze required values of drawdown impeller speed n_{JD} for mechanically agitated suspension of floating particles.
2. Standard deviation criterion σ constitutes useful measure to determine suspension homogeneity in the volume of the agitated vessel.
3. Values of the standard deviation σ decrease with the increase of the impeller speeds n resulting in the increase of the suspension homogeneity. The state of the particles dispersion in the suspension corresponding to the impeller speed somewhat higher than just drawdown impeller speed n_{JD} provides sufficient homogenization of the system. For many technologies, such suspension homogeneity is acceptable. Completely homogenized suspension, reached for much higher impeller speed than n_{JD}, is characterized by small values of the standard deviation σ, but high energy consumption.

References

[1] Stręk F., *Mieszanie i mieszalniki*, WNT, Warsaw 1981.
[2] Kamieński J., *Mieszanie układów wielofazowych*, WNT, Warsaw 2004.
[3] Etchells A.W., *Mixing of floating solids*, Plenary Lecture, 4th Intern. Symp. on Mixing in Industrial Processes ISMIP 4, Toulouse, France, 14–16.05.2001.
[4] Ozcan-Taskin G., Wei H., *The effect of impeller-to-tank diameter ratio on draw down of solids*, Chem. Eng. Sci., vol. 58, 2003, 2011-2022.
[5] Karcz J., Mackiewicz B., *Suspending of floating solids in an agitated vessel*, Chem. Proc. Eng., vol. 27, 2006, 1517-1533.
[6] Karcz J., Mackiewicz B., *An effect of particles wettability on the draw down of floating solids in a baffled agitated vessel equipped with a high-speed impeller*, Chem. Proc. Eng., vol. 28, 2007, 661-672.
[7] Mackiewicz B., PhD Thesis, Szczecin University of Technology, 2008.
[8] Karcz J., Mackiewicz B., *Effects of vessel baffling on the drawdown of floating solids*, Chem. Pap., vol. 63(2), 2009, 164-171.
[9] Ozcan-Taskin G., *Effect of scale on the draw down of solids*, Chem. Eng. Sci., vol. 61, 2006, 2871-2879.

[10] Murthy B.N., Ghadge R.S., Joshi J.B., *CFD simulation of gas-liquid-solid stirred reactor: Prediction of critical impeller speed for solid suspension*, Chem. Eng. Sci., vol. 62, 2007, 7184-7195.
[11] Mackiewicz B., Karcz J., *CFD modelling of suspension of floating particles*, Chem. Proc. Eng., vol. 30, 2009, 111-123.
[12] Cekinski E., Giuletti M., Seckler M.M., *A new approach to characterize suspensions in stirred vessel based on computational fluid dynamics*, Brazilian Journal of Chemical Engineering, vol. 27(2), 2010, 265-273.
[13] Tamburini A., Cipollina A., Micale G., *CFD simulation of solid – liquid suspension in baffled stirred tans below complete suspension speed*, Chem. Eng. Trans., vol. 24, 2011, 1435-1440.
[14] Karcz J., Kacperski Ł., Bitenc M., Domański M., *An application of computational fluid dynamics method to localization of regions of varied mixing intensity in mechanically agitated suspension of floating solids (in Polish)*, Przemysł Chemiczny, vol. 90(9), 2011, 1647-1650.
[15] Karcz J., Kacperski Ł., *An effect of grid quality on the results of numerical simulations of the fluid flow in an agitated vessel*, 14th European Conference on Mixing, Warsaw, Poland, 1–13.09.2012, 205-210.
[16] Kacperski Ł., Karcz J., *Numeryczna analiza rozkładu stężenia cząstek lekkich w zawiesinie mieszanej mechanicznie*, Inż. i Ap. Chem., vol. 52(4), 2013, 328-329.
[17] ANSYS CFX-Solver modeling guide, ANSYS Inc., Release 13.0, November 2010.